Bioactive glass coupling with natural polyphenols: Surface modification, bioactivity and anti-oxidant ability

Bioactive glass coupling with natural polyphenols: surface modification, bioactivity and anti-oxidant ability

Martina Cazzola[1], Ingrid Corazzari[2,3], Enrico Prenesti[2], Elisa Bertone[1], Enrica Vernè[1], Sara Ferraris[1]

[1] Politecnico di Torino, Department of Applied Science and Technology, Institute of Materials Physics and Engineering, C.so Duca degli Abruzzi 24, Torino, 10129, Italy.

[2] Università degli Studi di Torino, Department of Chemistry, Via Pietro Giuria 7, Torino, 10125, Italy.

[3] Centro Interdipartimentale "G. Scansetti" per lo studio degli amianti e di altri particolati nocivi, Via Pietro Giuria 9, 10125, Torino, Italy.

Corresponding author

Enrica Vernè

Phone: 0039-0110904717

Fax: 0039-0110904624

e-mail: enrica.verne@polito.it

Abstract

Polyphenols are actually achieving an increasing interest due to their potential health benefits, such as antioxidant, anticancer, antibacterial and bone stimulation abilities. However their poor bioavailability and stability hamper an effective clinical application as therapeutic principles. The opportunity to couple these biomolecules with synthetic biomaterials, in order to obtain local delivery at the site of interest, improve their bioavailability and stability and combine their properties with the ones of the substrate, is a challenging opportunity for the biomedical research.

A silica based bioactive glass, CEL2, has been successfully coupled with gallic acid and natural polyphenols extracted from red grape skins and green tea leaves. The effectiveness of grafting has been verified by means of XPS analyses and the Folin&Ciocalteu tests. In vitro bioactivity has been investigated by soaking in simulated body fluid (SBF). Surface modification after functionalization and early stage reactivity in SBF have been studied by means of zeta potential electrokinetic measurements in KCl and SBF. Finally the antioxidant properties of bare and modified bioactive glasses has been investigated by means of the evaluation of free radical scavenging activity by Electron Paramagnetic Resonance(EPR)/spin trapping technique after UV photolysis of H_2O_2 highlighting scavenging activity of the bioactive glass.

Keywords: bioactive glass, polyphenols, bioactivity, antioxidant activity

1. Introduction

An increasing interest in natural molecules has been registered in the last years in various application fields such as functional foods, cosmetics, pharmaceuticals, packaging and medicine due to their potential health benefits and low toxicity. Moreover, natural molecules can be obtained from wastes of food and beverages production chains and constitute a challenging approach for a green use of resources.
Among natural molecules, polyphenols obtained high attention because of their antioxidant, anti-inflammatory, antibacterial, bone stimulating and anticancer properties [1-3]. These molecules have been widely explored by direct application in *in vitro* and *in vivo* studies. The main drawbacks associated to polyphenols, that limit their effective application in medicine, are their relative low stability (mainly in neutral and basic media) and poor bioavailability when administered by conventional systemic routes. However polyphenols are stable in acid environment as the one presents in the initial stage of bone healing process [4, 5].
Some attempts to couple polyphenols with various materials have been reported in the literature with the aim to impart the specific properties of the biomolecules to the synthetic surface.
As far as pure polyphenols and model molecules are concerned, two flavonoids (taxifolin and quercetin) have been covalently immobilized onto titanium substrates [6, 7]; Pyrogallol 2-aminoethane has been used as model molecule for plant flavonoids for the functionalization of various polymeric, metallic and ceramic substrates [8]; quercetin and rutin have been coupled with mesoporous silica [9,10]; gallic acid has been grafted to zein fibers [11], and bioactive glasses were functionalized with chitosan [12-14], dendrimers [15], Mg/Al layered double hydroxide [16], magnetite and gold nanoparticles [17, 18], soybean peroxidase [19] and curcumin [20].
Considering polyphenol containing natural extracts, polyphenol coatings on various polymeric, metallic and ceramic substrates have been obtained from red wine, cacao and green tea extracts, in order to impart antibacterial and antioxidant properties [21] and apple polyphenols have been encapsulated into β-cyclodextrin nanosponges [22].
In previous research works, the authors investigated the grafting of gallic acid and polyphenols extracted from grape skin to bioactive glasses with various reactivity [23, 24] and of gallic acid to a bioactive and ferrimagnetic glass ceramic [25] exploiting hydroxyl groups exposed on the glass surface without any coupling/spacer molecule.
In the present work an in-depth study of the grafting of gallic acid, used as model molecule because of its simple structure, and polyphenols extracted from red grape skin and green tea leaves is reported, focusing the attention on the functionalization of a bioactive glass (named CEL2) that, in previous researches, revealed high reactivity and functionalization ability both in bulk and powder form. An optimized grafting procedure has been developed in order to obtain an effective grafting able to maintain the biomolecule

activity. Polyphenols presence and redox activity have been verified by means of both XPS technique and Folin&Ciocalteu analysis directly on the glass surface. For the first time, the effect of polyphenols on *in vitro* bioactivity and radical scavenging ability has been investigated and reported.

2. Materials and methods

2.1 Samples preparation

The bioactive glass developed and fully characterized in previous works [26-28], was used as substrate in the present research work, both in bulk and powder form.

The glass was produced by the traditional melt and quenching method and its molar composition is: 45% SiO_2, 3% P_2O_5, 26% CaO, 7% MgO, 15% Na_2O, 4% K_2O, with a 4:1 Na_2O/K_2O ratio [26-29].

The glass was obtained by melting the precursors (SiO_2, $Ca_3(PO_4)_2$, $CaCO_3$, $(MgCO_3)_4Mg(OH)_2 5H_2O$, Na_2CO_3 and K_2CO_3, >99%, Sigma Aldrich) in a platinum crucible at 1500°C for 1 hour. In order to obtain powder samples, the melted glass was poured in water obtaining a frit. The frit was milled and sieved up to grain size lower than 20 µm. The bulk samples were produced pouring the melted glass on a brass plate, the bars obtained were annealed in a furnace at 500°C for 13 hours in order to release residual stresses. After the annealing, the bars were cut with an automatic cutter in pieces 1 mm thick (Struers Accutom 5) and the slices obtained were polished with SiC abrasive papers (120-4000 grit) in order to achieve homogeneous surface. Glass slices with total area of 124,63 ± 13,88 mm^2 and 4,68 ± 0,03 g weight were obtained, while the powder samples were composed by 100 mg of glass powder in conformity with previous works [23, 24].

2.2 Phenol compounds handling

The biomolecules employed for the functionalization of the samples were gallic acid (3, 4, 5-Trihydroxybenzoic acid, GA), as model molecule, and polyphenols extracted from green tea leaves (TPH) or red grape skin (GPH) (Table 1).

The green tea leaves (Longjing variety) were imported from Hangzhou, China, dried in oven at 60°C and ground into very small pieces in a ceramic mortar.

For the conventional solvent extraction [29] a water-ethanol solution (20:80 volume ratio) with a solid-liquid ratio 1:50 was used. The extraction was conducted at the temperature of 60°C for one hour in a thermostatic bath. The extraction solution was separated from the tea leaves by filtering and then put into an incubator at 37°C until total ethanol solution evaporation.

Finally, the extract was collected and re-suspended in double-distilled water and freeze dried. .

Extract of red grape skin was obtained from red grape (Barbera variety) provided by a small-scale producer in the north-west of Italy (vineyard situated in Vaglio Serra, Asti, Piedmont, Italy).

The fresh grape skins were separated from the others parts of the grape and dried in an oven at 60°C and then milled in small pieces, as described in [24].
A conventional solvent extraction [30, 31] using a water-ethanol solution (20:80 volume ratio) with a solid-liquid ratio 1:20 was performed [24], in the same way of the one made for the tea leaves.

2.3 Glass surface activation

Free hydroxyl groups on the surface of the glass are necessary in order to effectively functionalize its surface [23, 24]. The method of exposition of the –OH groups for CEL2 was previously optimized by the authors' research group [27, 28]. In brief, the samples were washed in acetone in an ultrasonic bath for 5 minutes, to remove the surface contaminants, and then washed 3 times for 5 minutes in double-distilled water in order to expose –OH groups. The samples with the surface activated will be called glass-washed from now on (Table 1).

2.4 Surface functionalization

Stock solutions of gallic acid and natural extracts were prepared for glass functionalization: 1.0 mg/ml of GA (GA 97.5–102.5% titration, Sigma Aldrich) in double-distilled water, 1.0 mg/ml of TPH in double distilled water and 5.0 mg/ml of GPH in double distilled water.
Each sample (glass slices with area 124,63±13,88 mm^2 and weight 4,68 ±0,03 g for bulk samples and 100 mg for powder samples) was put in a holder coated with aluminum foil, in order to avoid UV degradation of the polyphenols, immediately after the procedure of activation, without drying, covered with 5 ml of the solution of functionalization and incubated for 3 hours at 37°C. After the incubation the samples were washed two times in double-distilled water, dried at room temperature and then preserved in the dark.
This protocol of functionalization was developed from previous works of the research group [23, 24] reducing the time of incubation with the scope of containing the ion release from the bioactive glass, that could induce an excessive pH increase, and the time of permanence of polyphenols at neutral/basic pH, reducing the consequent molecules degradation in the absence of a pH-metric buffer.
The samples grafted with polyphenols will be named CEL2+GA, CEL2+TPH and CEL2+GPH (Table 1).

2.5 Photometric analysis

Photometric determinations in the visible spectral region (CARY 500 Varian) were conducted on the functionalization solution before and after the samples soaking and on the samples themselves using the Folin&Ciocalteu method [23, 24] in order to evaluate the polyphenols concentration and depletion after surface grafting. 2 ml of the solution were mixed with 6 ml of double-distilled water and with 0,5 ml of Folin&Ciocalteu reagent (Folin&Ciocalteu phenol reagent, Sigma Aldrich). After 3 minutes 1,5 ml of 20%

(p/V) Na_2CO_3 solution were added and after 2 h of reaction the photometric measurement was carried out at 760 nm [23, 24].

A modified Folin&Ciocalteu method was utilized to quantify the polyphenols grafted on the surface of the samples. The functionalized samples was put into a holder and then covered with 8 ml of water, 0,5 ml of Folin&Ciocalteu reagent and 1,5 ml of 20% (p/V) Na_2CO_3 solution [25].

To quantify the amount of polyphenols, a standard calibration curve was prepared using solutions with different concentrations of GA (namely, 0,0025, 0,005, 0,01, 0,02, 0,03 and 0,04 mg/ml) as described in [23].

For this type of analysis were prepared at least three bulk and three powder samples of CEL2 washed, CEL2 + GA, CEL2 + GPH and CEL2 + TPH.

2.6 XPS analysis

X-ray Photoelectron Spectroscopy analysis (XPS, PHI 5000 VERSAPROBE, PHYSICAL ELECTRONICS) was employed to evaluate the presence of the polyphenols on the surface of the samples.

For this analysis one bulk sample per type (CEL2 washed, CEL2+GA, CEL2+GPH and CEL2+TPH) was analyzed . The chemical composition of the surface was investigated by means of survey spectra and the chemical state of C and O were further determined by high resolution spectra in order to determine the presence of chemical groups characteristic of the activated surfaces or of the grafted biomolecules.

2.7 Apatite-forming ability tests

To compare the apatite-forming ability (bioactivity) of glass before and after functionalization, the samples were soaked in simulated body fluid (SBF) with the composition reported in Table 2 [32, 33]. The samples, one for each type (CEL2 washed, CEL2+GA, CEL2+GPH and CEL2+TPH), both bulk and powder, were put in a bottle coated with aluminum foil, for preserving polyphenols degradation by UV, and covered with 25 ml of SBF. The amount of the SBF used was chosen for the bulk samples according with Kokubo and Takadama [34] considering both the top and the bottom surfaces. Regarding the powder samples, because of the difficulty in the determination of the surface area due to the high reactivity of the glass, 25 ml of SBF were used according with previous works [23, 24]. The samples were incubated at 37°C up to 14 days. Every 3 days a refresh of the solution was made and the pH was measured to control eventual variation of the SBF pH due to the ionic release from the glass surface. After the soaking in SBF the samples were dried at room temperature under the hood. The deposition of hydroxyapatite on the surface was analyzed after 7 and 14 days by means of Field Emission Scanning Electron Microscopy equipped with Energy Dispersive Spectroscopy (FESEM-EDS SUPRATM 40, Zeiss and Merlin Gemini Zeiss).The samples before this analysis were sputtered coated after the drying with a thin Cr -layer in order to make them conductive.

The samples were also analyzed after 3, 7 and 14 days by means of FTIR (FTIR Alpha, Bruker Optics, Ettlingen, Germany) on pellets of the samples obtained with KBr (titration ≥99,0%, Sigma Aldrich) and glass powders.

2.8 Contact angle measurements

The samples were placed with the washed or functionalized side facing upward on the support of a heating microscope (Misura®, Expert System Solutions), working at room temperature. A drop (5 µl) of double-distilled water was deposited with a micropipette on the surface. The water drop images were acquired with the microscope software and elaborated with Image J (1:47 version) software for the determination of contact angle.

This analysis was performed four time for each type of functionalization in order to evaluate the variation of the surface wettability that is induced by the functionalization of the sample.

2.9 Zeta potential measurements

Surface charge of CEL2 samples, before and after functionalization, was determined by means of electrokinetic measurements (SurPASS, Anton Paar). For this analysis a couple of samples was prepared for each type (CEL2 washed, CEL2+GA, CEL2+GPH and CEL2+TPH) and four measurements were run on each couple. The surface zeta potential was determined in function of pH in a 0,001 M KCl electrolyte solution varying the solution pH by addition of 0,05M HCl or 0,05M NaOH through the instrument automatic titration unit. A new couple of samples were employed for measurement in the acid or basic range in order to avoid artifacts due to surface reactivity in the electrolyte.

In order to monitor the reactivity of bare and functionalized CEL2 samples in Simulated Body Fluid zeta potential measurements in SBF were performed. The electrolyte solution was prepared by means of drop by drop addition of SBF to water up to a pH of about 7.5 and a conductivity close to 15 mS/m. Measurements in SBF were performed without pH titration but they were repeated for 20 cycles (at about 70 min each) in order to monitor early stage surface reactivity of the surfaces in contact with physiological fluids.

2.10 Evaluation of free radical scavenging activity

The evaluation of free radical scavenging activity was performed for glass powder samples both washed and functionalized. This analysis was carried out in duplicate through Electron Paramagnetic Resonance (EPR)/spin trapping technique after UV photolysis of H_2O_2 [35-37].

The glass powder (15 mg) was placed in a quartz cuvette 100 µl of deionized H_2O, then, with the suspension under magnetic stirring, 100 µl of saline buffer 0,5M, 200 µl of DMPO (5,5-Dimethyl-1-pyrroline-N-oxide) 0,17 M and 100 µl of H_2O_2 0,002M were added . The suspensions, continuously stirred,

were irradiated with a UV lamp with a cut-off filter at 315 nm in order to cause the photolysis of H_2O_2 preventing the photo-degradation of DMPO. After 5, 10 and 30 minutes of irradiation aliquots of suspension (50 µl) were collected and the EPR spectra recorded with an X-band EPR spectrometer (Miniscope 100, Magnettech, Germany).

The same experiment was carried out on a blank solution without glass powder (positive control).

The intensity of the signal obtained is proportional at the radical present in solution. The signals were double-integrated and the values obtained expressed as arbitrary units. The EPR/spin trapping data and figures are provided as mean ±SD. The results were analyzed by Student t-test. $P<0,05$ was considered significant.

3. Results and discussion

3.1 Macroscopic observation and pH measurements

The color of the samples changes after the treatment from colorless to brown for GA functionalization, to yellow for GPH functionalization and to orange for TPH functionalization. A color change can be evidenced also for the functionalization solutions and is reported in Table 3. The pH values of both the functionalization and uptake solutions were measured (the term "uptake solutions" refers to the functionalization solutions after soaking of the samples for the time defined by the protocol) and their color was observed, as an indication of the possible chemical alterations of the biomolecules. The pH is an important parameter because the polyphenols are sensitive to its changes and it has been reported that they begin to degrade at pH values above 7.4 [4].

The starting solutions of functionalization are characterized by a fairly acid pH and during functionalization an alkalization of the uptake solutions can be observed.

The alkalization of all uptake solutions is due to the CEL2 reactivity in aqueous media. As widely reported in the literature [38, 39], in an aqueous environment the silica amorphous network of bioactive glasses reacts with water with consequent breakage of the oxygen bridges and formation of radicals -OH. Furthermore the ion exchange between the Na^+ ions of the glass and H_3O^+ of the aqueous solution promotes the formation of the radicals -OH. Acid solutions, such as those used for the functionalization, increase the ion exchange phenomenon [27].

The glass powder has greater surface area than the bulk, and this is the reason why a higher ion exchange in solution can occur, with a consequent higher increase in the solution pH, as reported in Table 3.

In the present work, the functionalization time has been reduced to 3h, compared to the 24h used in previous reports [23, 24], in order to better control the glass and solution reactivity and avoid molecular alterations. Moreover shortening of the functionalization time allows to reduce the time of permanence of the biomolecules at neutral/basic pH reducing the risk of degradation and improving the stability and the

amount of the bonded biomolecules. As far as the bulk samples the values of pH for uptake solutions is significantly lower than the ones reported in previous papers by the authors [23, 24].
It has been suggested that the pH of the solutions should remain about 7.4 because this is known as the threshold at which begins the transformation of the catechol groups in quinones, which have a typical dark coloration [40, 41]. The dark color observed on functionalized samples can be explained with this phenomenon. The more intense color of the samples functionalized with the GA and of the solutions of uptake of CEL2 + GA powder is due to the highly sensitivity to pH shift of GA phenols groups. On the other hand the extracts from grape and tea are composed of different polyphenols not all sensitive to the same manner to the environment alkalization [4].

3.2 Photometric analyses

The standard calibration curve was obtained measuring the absorbance at 760 nm of standard GA solutions after the Folin&Ciocalteu reactions, as reported in [23]. The curve obtained has a good linear relationship and a good coefficient of correlation (R^2=0, 9991) and trough the equation derived from this curve (y=23,97x + 0, 0047 were y is the absorbance at 760 nm end x the concentration) it is possible to determine the concentration of the polyphenols in GA equivalents [mg/ml]. For GPH and TPH the concentration is expressed as mg/ml of total polyphenols in the mixture of the natural extracts. Total polyphenols have been quantified comparing the UV absorbance at 760 nm of the sample and the calibration curve obtained with standard solutions of gallic acid. The method is based on the assumption that all the polyphenols react as gallic acid in the Folin&Ciocalteu redox reaction, this is the reason why their concentration is defined as “gallic acid equivalents”. Really, a concentration is measured on the basis of a common reactivity. GA, GPH and TPH solutions were analyzed before and after the functionalization procedure with UV spectrometric measurements after reaction with Folin&Ciocalteu reagent, in order to compare the concentration of the polyphenols in the starting solutions end their consumption after the surface grafting.
Figure 1a shows the concentration in GA equivalents units (mg/ml) of polyphenols in solution, before and after the functionalization. It can be observed that the concentration of polyphenols is significantly lowered for the uptake solutions with respect to the stock solution. The effect is wider for powder than for bulk samples. This result is in accordance with the surface grafting of a certain amount of molecules during the functionalization process, and with previous results by the authors [23, 24].
The larger decrease of the polyphenols in the uptake solution of powder samples can be attributed to the greater surface area exposed by these samples that may allow to graft a higher amount of polyphenols. It must be taken into account that the concentration lowering can be in part attributed also to molecular alterations related to the previously discussed basification of the solutions. For this reason it is extremely important to evaluate concentration and activity of polyphenols directly onto the material surface.

As described in the materials and methods section and in [25], the Folin&Ciocalteu method has been adapted in order to evaluate the concentration of polyphenols on the surface of bioactive glasses both in bulk and powder forms. Results are reported in Figure 1b in GA equivalents units of the biomolecules on the surface of CEL2 samples functionalized with GA, GPH and TPH. A certain amount of GA, GPH and TPH has been recorded on both bulk and powder CEL2 samples. This result is significant because it highlights that polyphenols are present on the material surface and are able to maintain their activity after grafting. For all the three types of molecules, the concentration of polyphenols is higher on the powder samples due to their greater surface area. The samples soaked in GPH solution show a lower concentration because the original functionalization solution contained a lower amount of polyphenols (Figure 1a).
It can be observed that for GA the concentration of the bare solution is close to the nominal one and it results higher than the one of natural polyphenols (GPH and TPH). This result can be explained considering that GA is a pure molecule while GPH and TPH are natural extracts and their complex composition is not fully known. These observations are in accordance with previous results from the authors [23, 24].

3.3 XPS analysis

XPS analysis was performed on bulk samples in order to verify the presence of the polyphenols (by means of the observation of their characteristic chemical functionalities) on the surface.
Table 4 shows atomic percentages of the elements detected on the surface of CEL2 samples at different steps of the functionalization process.
A decrease of the percentage of the glass constituents (calcium, sodium, potassium and phosphorus) can be observed after the functionalization procedure. This phenomenon confirms the ionic exchange between the glass surface and the solution of functionalization discussed in the paragraph 3.1.
The variation on the percentage of calcium, sodium and potassium for the functionalized samples can be attributed to the ionic exchange and to the ability of the polyphenols to bind some metal ions. It is known that GA has great complexing ability for calcium ions [43]. So it is not surprising that, after soaking into the GA functionalization solution, a higher amount of calcium ions can be released in comparison to sodium ones. The lower calcium decrease following the functionalization with GPH and TPH can be correlated to the fact that, in these extracts, GA is not pure, but it is present in lower amounts, since the natural extract contains a mixture of different polyphenols. In these solutions the sodium and calcium release is more related to their mobility in the glass network rather than to the complexing ability of the solutions.
Potassium is present in very low amount in the glass, so it is not surprising that in all the solutions it has been completely released. A significant increase in the carbon content can be observed after GPH and TPH grafting on CEL2 surface but not after GA grafting. This phenomenon can be explained considering both the substitution of surface carbonates after functionalization and also the bigger dimension of natural

polyphenols compared to pure GA and consequent higher carbon content. A variation of the percentage of carbon and oxygen, of which polyphenols are rich, can also be noted.

The simple observation of the chemical elements on the surface is not sufficient to determine the presence of the biomolecules. In order to detect the specific chemical groups of polyphenols the detailed analyses of carbon and oxygen regions have been performed and reported in figures 2 and 3 respectively.

The high resolution XPS spectra of carbon region for bare and functionalized CEL2 samples are reported in Figure 2. As far as the washed sample is concerned (Figure 2(a)) signals at 284,79 eV and 289,25 eV can be observed. The first signal can be attributed to the hydrocarbon contaminations that are unavoidable for reactive surfaces [10, 11, 12] and have been already observed by the authors on CEL2 samples [23, 24, 44]. The second signal can be attributed to carbonates, frequently observed on the surface of bioactive glasses [45] as contaminants and already highlighted by the authors on CEL2 after washings [23, 24]. The signal of carbonates disappears after the functionalization process with all the considered molecules (Figure 2 (b, c, d)), as previously observed by the authors [23, 24]. On the other hand, the signal at about 284,8 eV persists on all the samples after functionalization (Figure 2(b, c, d)). Since the signal highlights the presence of C-C and C-H bonds, it can be attributed to both surface contamination and also to C-C and C-H bonds in the polyphenols molecules after their grafting. Their increase on the surface of CEL2+GPH and CEL2+TPH can be correlated to the increase of the atomic percentage of carbon on the surface of the functionalized samples with natural polyphenols. After the functionalization two characteristics signals appears on the surface of CEL2 samples grafted with GA, GPH and TPH: one at about 286 eV and the other at about 288 eV. These signals can be attributed to C-O and C=O bonds respectively [46] and have been already observed by the authors on CEL2 modified with polyphenols [23, 24]. C=O and C-OH bonds are abundant in polyphenols and can confirm the presence of these molecules on the material surface. Moreover, the peak of C=O group can be correlated also with the tendency of GA to oxidize into a quinone form in basic environment [23].

The high resolution spectra of the oxygen region for bare and functionalized CEL2 samples are reported in Figure 3. Looking at the washed sample (Figure 3 (a)), three main contributions can be detected: one at 527,93 eV, one at 530,34 eV and the last one at 531,69 eV. They can be attributed to the oxides present in the composition of the glass, silica and –OH groups respectively [47, 48].

After the functionalization with GA, GPH and TPH the oxygen region still presents three main contributions (Figure 3(b, c, d)). A moderate shift to higher energies can be underlined for the OH signals after the functionalization and can be attributed to the higher energy usually associated to OH in phenolic groups [44]. After functionalization the signals at about 529 eV can be attributed to both oxides and C=O bonds, while the one at about 531 eV can be attributed to both silica and C-O bonds, as already observed on CEL2 functionalized with polyphenols [23, 24].

3.4 Apatite-forming ability tests

Bulk and power glass samples were soaked in SBF [32, 33] up to 14 days in order to evaluate their in vitro apatite-forming ability (bioactivity). Surfaces have been analyzed by means of Field Emission Scanning Electron Microscopy equipped with Energy Dispersive Spectroscopy and Fourier Transformed InfraRed Spectroscopy in order to investigate surface reactivity and hydroxyapatite precipitation.

PH measurements during the soaking period indicate values of at about 7.6 for bulk samples and 7.9 for powder ones. The reported values are included in the physiological tolerability range and evidence a good ability of SBF to buffer alkalization.

Powder samples were analyzed after 3, 7 and 14 days by means of FTIR and after 7 and 14 days by mean of Field Emission Scanning Electron Microscopy.

The IR spectra of CEL2 powders (bare/functionalized) at different times of SBF soaking are reported in Figure 4. The spectra were performed in transmission on pellets of powder samples and KBr and three acquisitions for each spectrum were made. The presence of hydroxyapatite on samples through IR spectra is principally shown by a double peak around 600 cm^{-1} and 560 cm^{-1} that are correlated with the bending vibration of P-O bonds and by the intensification of the peak at 1025 cm^{-1} due to the phosphate stretching vibration in the apatite structure[49-53]. After 3 days these signals begin to appear only for the samples functionalized with GA while after 7 days these peaks are clearly present and well defined for functionalized samples but not for the non-functionalized one. After 14 days hydroxyapatite seems to be presents in all the tested samples.

FESEM images of CEL2 bulk samples, after different periods in SBF, are reported in figure 5.

A lot of precipitates can be observed on all the surfaces after 7 days of soaking in SBF. EDS reported in Table 5a confirm the presence of Ca and P in these precipitates and the ratio of this two elements (Table 5b) is comparable with that of stoichiometric Hap (1,67) [54]. However at 7 days the Si signal is still evident on CEL2 washed samples while it is hindered on functionalized ones. After 14 days of soaking a uniform Ca-P rich layer can be observed on all the surfaces. These results confirm a faster hydroxyapatite kinetics deposition for polyphenols functionalized CEL2 samples. It can be also noted a little difference in the HAp morphology between bare and functionalized CEL2 substrates. This difference is clearly visible in Figure 5, where the FESEM micrographs of bulk samples are reported. The characteristic “cauliflower-like” structure can be observed for the non-functionalized samples, while different structures were obtained for the functionalized samples. A globular structure is shown by the HAp on the samples functionalized with TPH and it is more visible after 7 days because after 14 the “globes” are grown and are attached one to each other. The samples functionalized with GPH exhibits a very compact “carpet-like” structure that becomes thicker after 14 days. The GA functionalization gives to the HAp that grown on the samples a “column-like” structure that becomes evident after 14 days of soaking.

It has been reported that polyphenols are able to regulate the precipitation and the morphology of HAp crystals and can participate at the nucleation and at the mineralization process. This can be attributed to the ability of the phenolic hydroxyls to interact with Ca^{2+} ions and the complex polyphenol-HAp may connect by means of intermolecular forces [43, 55].

3.5 Contact angle measurements

The mean values of the contact angles and their standard deviations are shown in Figure 6.

For the CEL2 washed sample a contact angle of 8,1 ± 0,7 ° was obtained, that is indicative of a highly wettable surface due to the presence of the hydroxyl groups exposed on the surface [28].

A low contact angle indicates the success of the procedure of surface activation implemented to expose the hydroxyl groups.

A contact angle of 5,3 ± 0,7 ° has been measured on the sample of CEL2 functionalized with GA, evidencing, a slight increase of the surface wettability compared to the washed glass. This increase in wettability is attributable to the hydroxyl groups exposed by the GA [56].

For the samples of CEL2 functionalized with GPH and TPH the following values were obtained: 35,2 ± 1,4 ° for the CEL2 + GPH and 37,7 ± 5,1 ° for the CEL2 + TPH.

The samples functionalized with GPH and TPH are less wettable than the sample of CEL2 washed and this can be explained by the greater complexity of the polyphenols present in these extracts that have longer alkyl chains and they can expose groups $–CH_3$ which reduce the wettability of the surface [8].

3.6 Zeta potential measurements

Zeta potential measurements in function of electrolyte pH are reported in Figure 7 and a summary of the obtained data in Table 6.

It can be observed that all the surfaces present an isoelectric point in the acidic range and consequently they are all negatively charged at physiological pH. However, a defined value for the isoelectric point has been determined only for the washed CEL2 sample. In the other cases surfaces evidenced a strong reactivity with the solution in the acidic range and it was not possible to reach the 0 values without artifacts. Looking at the graphs it can be deducted that all the surfaces have an isoelectric point close to 3 and comparable with the one of CEL2 washed and to the one of silica (2,5-3,5) [57-59]. A plateau in the surface charge can be observed for all the surfaces in the basic range (Figure 7 a). It can be ascribed to the presence of acidic hydroxyl groups on the surface [60]. The result is consistent with the surface activation step for the CEL2 washed sample and with polyphenols grafting for CEL2+GA, CEL2+GPH and CEL2+TPH ones. Moreover, it is in accordance with FTIR and XPS observations discussed in the previous paragraphs.

Looking at the zeta potential measurements in SBF (Figure 7 b), it can be observed that the surface charge in physiological solution is negative, as previously observed at physiological pH in KCl electrolyte solution.

A moderate increase in the solution pH can be noted after 20 cycles, confirming the reactivity of bare and modified glasses in contact with aqueous media (ion exchange). This increase is more evident for CEL2+GPH and CEL2+TPH samples compared to CEL2 washed and CEL2+GA ones. A significant decrease in the negative surface charge can be observed for all the samples after 20 cycles. This variation is more evident for CEL2 washed and CEL2+GA samples. The variation of the surface charge through less negative values can be ascribed to the absorption of positive ions from the solution (mainly Ca^{2+}) during the first stages of the bioactivity mechanism. This result is in accordance with observations reported in the literature about the bioactivity mechanism of bioactive glasses [61, 62] and titanium surfaces [63, 64] investigated by means of zeta potential measurements. Moreover the results confirm the observation of hydroxyapatite precipitation after longer time soaking on SBF observed by means of FTIR and FESEM analyses.

3.7 Evaluation of free radical scavenging activity

In order to assess the antioxidant properties of CEL2 before and after the functionalization, the samples were suspended in a buffered solution in the presence of H_2O_2 and DMPO following the procedure described in [38]. The suspensions were irradiated with a mercury-xenon lamp (cut off 315_nm) to cause the photolysis of H_2O_2 with the production of HO. The capability of the bioactive glasses to scavenge HO• radical was assessed by means of EPR/spin trapping. A solution of H_2O_2 and DMPO without glass powder subjected at the same irradiation conditions was employed as positive control.

The signal intensities, obtained by double integration of the EPR spectra, are proportional to the concentration of HO•. Figure 8 reports the average signal intensities ± SD after 5, 10 and 30 minutes of irradiation of two independent experiments. At each time-point tested the signal recorded with all the active glass samples was significantly lower than the positive control (*$p < 0,05$). This result evidenced that all the tested samples exhibited a remarkable scavenging activity towards the HO• generated by photolysis of H_2O_2.

Unexpectedly CEL2 showed an intrinsic scavenging capability even without the presence of antioxidant molecules at the surface. The chemical mechanism at the basis of this behavior has not been yet clarified and will be the object of further investigation. As far as inorganic materials are concerned, in the literature [65, 66] antioxidant capacity has been reported for silica hydride.

The effect of the functionalization was assessed comparing the results obtained with the functionalized samples and those obtained with CEL2 washed. After 5 minutes of incubation the capability of CEL2 + TPH to scavenge HO• radicals was slightly, but significantly higher (#$p < 0.05$) than that exhibited by CEL2 washed. On the other hand no significant differences were detected among CEL2 and the functionalized samples (CEL2+GA and CEL2+GPH). After 10 and 30 minutes no significant difference among CEL2 and the functionalized samples were observed. These results indicate that TPH are the only effective polyphenols

to increase the scavenging capability of CEL2 among the molecules tested in these experimental conditions. The little increment of the bare glass ability of scavenging HO· radicals for samples modified with natural molecules, confirms the antioxidant activity of polyphenols [68-74]. The lack of antioxidant activity showed by GA and GPH at each time point tested and by TPH at longer times of irradiation may be due to their consumption following reaction with HO• or to decomposition due to exposure to UV light.

4. Conclusion

Gallic acid (as model molecule) and natural polyphenols extracted from red grape skins (GPH) and green tea leaves (TPH) have been successfully grafted to the surface of a bioactive glass (CEL2) without the use of any synthetic spacer. The presence and activity of the biomolecules on the glass surface have been verified by means of XPS analyses and the Folin&Ciocalteu test. A faster in vitro bioactivity (ability to induce hydroxyapatite precipitation in SBF) has been observed for the functionalized bioactive glass. Moreover a variation of hydroxyapatite shape has been noted varying the grafted biomolecule. Zeta potential measurements confirmed the surface modification processes after functionalization as well as the surface reactivity in SBF. Free radical scavenging activity evaluation evidenced for the first time a certain antioxidant activity of the bare bioactive glass that is improved by the grafting of tea polyphenols.
The investigation of the biological response (healthy/cancer cells and bacteria) to the here described functionalized bioactive glasses is actually in progress and will be discussed in a future paper.
The results of the present research suggest that bioactive glasses functionalized with natural polyphenols can be promising materials for bone contact applications in critical situations such as poor bone quality/quantity, cancer and infections.

Acknowledgments

Dr. Carmagnola Irene and Dr. Ruini Francesca (Politecnico di Torino, Department of Mechanical and Aerospace Engineering) are kindly acknowledged for freeze-drying facilities.
Italian Ministry of Education, Universities and Research (MIUR, "Fondo per il sostegno ai giovani" 2012) is kindly acknowledged for funding PhD activities of one of the authors (M. Cazzola).

References

[1] Z.B. Lu, G.J. Nie, P.S. Belton, H.R. Tang, B.L. Zhao, Structure-activity relationship analysis of antioxidant ability and neuroprotective effect of gallic acid derivatives, Neurochem. Int. 48 (2006) 263–274.

[2] S. Quideau, D. Deffieux, C. Douat-Casassus, L. Pouysegu, Plant Polyphenols: Chemical properties, Biological activities and synthesis, Angew. Chem. Int Ed. 50 (2011) 586-621.

[3] L Bravo, Polyphenols: Chemistry, dietary sources, metabolism and nutritional significance, Nutr. Rev. 56 (1998) 317-333.

[4] M. Friedman, h. S. Jurgens, Effect of pH on the stability of plant phenolic compaunds, J. Agric. Food Chem. 48 (2000) 2101-2110.

[5] http://cal.vet.upenn.edu/projects/saortho/chapter_03/03mast.htm (accessed 26 October 2015, 11.23 a.m.)

[6] A. Cordoba, M. Satuè, M. Gomez-Florit, M. Hierro-Oliva, C. Petzold, S.P. Lyngstadaas, M.L .Gonzales-Martin, M. Monjo, J.M. Ramis, Flavonoid modified surfaces: multifunctional bioactive biomaterials with osteopromotive, anti-inflammatory and anti-fibrotic potential, Adv. Healthcare Mater. 4 (2015) 540-549.

[7] A. Cordoba, M. Satuè, M. Gomez-Florit, M. monjo, JM Ramis, Flavonoid coated titanium surfaces for bioactive bone implants, Stem. Cell Transl. Invest. 2 (2015) 520-524.

[8] S. Hong, J. Yeom, I.Tl Song, SM Kang, H. Lee, H. Lee, Pyrogallol 2-aminoethane: a plant flavonoid-inspired molecule for material-independent surface chemistry, Adv. Mater. Int. 1 (2014) 1400113.

[9] G. Berlier, L. Gastaldi, E. Ugazio, I. Miletto, P. Iliade, S. Sapino, Stabilization of quercetin flavonoid in MCM-41 mesoporous silica: positive effect of surface functionalization, J. Colloid Interface Sci. 393 (2013) 109-118.

[10] G. Berlier, L. Gastaldi, S. Sapino, I. Miletto, E. Bottinelli, D. Chirio, E. Ugazio, MCM-41 as a useful vector for rutin topical formulations: synthesis, characterization and testing, Int. J. Pharm. 457 (2013) 177-186.

[11] Y.P. Neo, S. Swift, S. Ray, M. Gizdavic-Nikolaidis, J. Jin, C.O. Perera, Evaluation of gallic acid loaded electrospun fiber mats as novel active packaging materials, Food Chem. 14 (2013) 3192-3200.

[12] Y.S. Cho, S.K. Kim, C.B. Ahn, J.Y. Je, Preparation, characterization and antioxidant properties of GA–grafted–chitosans, Carbohydr. Polym. 83 (2011) 1617-1622.

[13] W. Pasanphan, G.R. Buettner, S. Chirachanchai, Chitosan gallate as novel potential polysaccharide antioxidant: an EPR study, Carbohydr. Res. 345 (2010) 132–140.

[14] S.H. Yu, F.L. Mi, J.C. Pang, S.C. Jiang, T.H. Kuo, S.J. Wu, S.S. Shyu, Preparation and characterization of radical and pH–responsive chitosan–GA conjugate drug carriers, Carbohydr. Polym. 84 (2011) 794–80.

[15] A. Sharma, S. Prakash Gautam, A. K. Gupta, Surface modified dendrimers: synthesis and characterization for cancer targeted drug delivery, Bioinorg. Med. Chem. 19 (2011) 3341-3346.

[16] X. Kong, L. Jin, M. Wei, X. Duan, Antioxidant drugs intercalated into layered double hydroxide: Structure and in vitro release, Appl. Clay Sci. 49 (2010) 324-329.
[17] M.Y. Ghotbi, M.Z. bin Hussein, Controlled release study of anti–carcinogenic agent, gallate from the surface of magnetite nanoparticles, J. Phys. Chem. Solids. 73 (2012) 936-942.
[18] N.A. Moreno–Alvarez, G.A. Martinez–Castanon, N. Nino–Martinez, J.F. Reyes–Macias, N. Patino–Marin, J.P. Loyola–Rodriguez, F. Ruiz, Preparation and bactericide activity of GA stabilized gold nanoparticles, J. Nanopart. Res. 12 (2010) 2741-2746.
[19] V. Aina, D. Ghigo, T. marchis, G. Cerrato, E. Laurenti, C. Morterra, G. Malavasi, G. Lusvardi, L. Menabue, L. Bergandi, Novel bio-conjugate materials: soybean peroxidase immobilized on bioactive glasses containing Au nanoparticles, J. Mater. Chem. 21 (2011) 10970-10981.
[20] G. Malavasi, E. Ferrari, G. Lusvardi, V. aina, F. Fantini, C. Morterra, F. Pignedoli, M. Saladini, L. Menabue, The role of coordination chemistry in the development of innovative gallium-based bioceramics: the case of curcumin, J. Mater. Chem. 21 (2011) 5027-5037.
[21] T.S. Sileika, D.G. Barrett, R .Zhang, K.H.A. Lau, P.B. Messersmith, Colorless multifunctional coatings inspired by polyphenols found in tea, chocolate and wine, Angew. Chem. Int. Ed. 52 (2013) 10766-10770.
[22] M. Ramirez-Ambrosi, F. caldera, F. trotta, L.A. Berrueta, B. Gallo, Encapsulation of apple polyphenols in β-CD nanosponges, J. Inc. Phenom. Macrocycl. Chem. 92 (2014) 80-85.
[23] X. Zhang, S. Ferraris, E. Prenesti, E. Vernè, Surface functionalization of bioactive glasses with natural molecules of biological significance, Part I: Gallic acid as model molecule, Appl. Surf. Sci. 287 (2013) 329-340.
[24] X. Zhang, S. Ferraris, E. Prenesti, E. Vernè, Surface functionalization of bioactive glasses with natural molecules of biological significance, part II: Grafting of polyphenols extracted from grape skin, Appl. Surf. Sci. 287 (2013) 341-348.
[25] S. Ferraris, X. Zhang, E. Prenesti, I. Corazzari, F. Turci, M. Tomatis, E. Vernè, Gallic acid grafting to a ferrimagnetic bioactive glass-ceramic, J. Non-Cryst. Solids 432 (2016) 167-175.
[26] C. Vitale-Brovarone, E. Vernè, L. Robiglio, G. Martinasso, R.A. Canuto, G. Muzio, Biocompatible glass–ceramic materials for bone substitution, J. Mater. Sci. :Mater. Med. 19 (2008) 471-478.
[27] E. Vernè, C. Vitale-Brovarone, E. Bui, C.L. Bianchi, A.R. Boccaccini, Surface functionalization of bioactive glasses, J. Biomed. Mater. Res. 90A (2009) 981-992.
[28] E. Vernè, S. Ferraris, C. Vitale-Brovarone, S. Spriano, C.L. Bianchi, A. Naldoni, M. Morra, C. Cassinelli, Alkaline phosphatase grafting on bioactive glasses and glass–ceramics, Acta Biomater. 6 (2010) 229-240.
[29] Q. V. Vuong, J. B. Golding, C. E. Stathopoulos, M. H. Nguyen, P. D. Roach, Optimizing conditions for the extraction of catechins from green tea using hot water, J. Sep. Sci. 34 (2011) 3099-3106.
[30] T. Vatai, M.˘Skerget,˘Z. Knez, Extraction of phenolic compounds from elder berry and different grape marc varieties using organic solvents and/or supercritical carbon dioxide, J. Eng. 90 (2009) 246-254.

[31] Y.Cho, J. Hong, H. Sook Chun, S. K. Lee, H.Min, Ultrasonication-assisted extraction of resveratrol from grapes, J. Food Eng. 77 (2006) 725-730.
[32] T. Kokubo, H. Kushitani, S. Sakka, T. Kitsugi and T. Yamamuro, Solutions able to reproduce in vivo surface-structure changes in bioactive glass-ceramic A-W, J. Biomed. Mater. Res. 24 (1990) 721-734.
[33] T. Kokubo, S. Ito, Z. T. Huang, T. Hayashi, S. Sakka, T. Kitsugi and T. Yamamuro, Ca,P-rich layer formed on high-strength bioactive glass-ceramic A-W, J. Biomed. Mater. Res., 24 (1990) 331-343.
[34] T. Kokubo, H. Takadama, How useful is SBF in predicting in vivo bone bioactivity?, Biomaterials 27 (2006) 2907–2915
[35] B.Fubini, L.Mollo, E.Giamello, Free radical generation at the solid/liquid interface in iron containing minerals , Free Rad. Res. 23 (1995) 593-614.
[36] I.Corazzari, S. Livraghi, S. Ferrero, E. Giamello, B. Fubini, I. Fenoglio, Inactivation of TiO2 nano-powders for the preparation of photo-stable sunscreens via carbon-based surface modification, J. Mater. Chem. 22 (2012) 19105-19112.
[37] I. Fenoglio, M.Tomatis, D. Lison, J. Muller, A. Fonseca ,J. B. Nagy , B. Fubini, Reactivity of carbon nanotubes: Free radical generation or scavenging activity?, Free Radical Biol. & Med. 40 (2006) 1227-1233.
[38] W. Cao, LL. Hench, Bioactive materials, Ceram. Int. 22 (1996) 493-507.
[39] LL. Hench, N. Roki, MB Fenn, Bioactive glasses: importance of structure and properties in bone regeneration, J. Mol. Struct. 1073 (2014) 24-30.
[40] Z. Yang, J. Wu, X. Wang, J.Wang, N. Huang, Inspired Chemistry for a Simple but Highly Effective Immobilization of Vascular Endothelial Growth Factor on Gallic Acid functionalized Plasma Polymerized Film, Plasma Process. Polym. 9 (2012) 718-725.
[41] Z. Yang, Y. Yang, W.Yan, Q. Tu, J. Wang, N. Huang, Construction of Polyfunctional Coatings Assisted by Gallic Acid to Facilitate Co-Immobilization of Diverse Biomolecules, ACS Appl. Mater. Interfaces 5 (2013) 10495-10501.
[42] C.H. Venkateswarlu, M. Ssnkar Das, V. T. Athavale, Studies of gallic acid complexes with metals and their analytical applications, Proceedings of the Indian Academy of Sciences - Section A 40 (1954) 260-269.
[43] B. Tang, H. Yuan, L. Cheng, X. Zhou, X. Huang, J. Li, Effects of gallic acid on the morphology and growth of hydroxyapatite crystals, Arch. Oral Biol. 60 (2015) 167-173.
[44] E. Vernè , S. Ferraris, C. Vitale-Brovarone, A. Cochis, L. Rimondini, Bioactive glass functionalized with alkaline phosphatase stimulates bone extracellular matrix deposition and calcification in vitro, Appl. Surf. Sci. 313 (2014) 372-381.
[45] http://www.xpsfitting.com/2011/03/c-1s-carbonates.html (accessed 22 July 2015, 8:51 a.m.)
[46] Y. P. Neo, S. Swift, S. Ray, M Gizdavic-Nikolaidis, J. Jin, C.O. Perera, Evaluation of gallic acid loaded zein sub-micron electrospun fibre mats, as novel active packaging materials, Food Chem. 141 (2013) 3192-3200.

[47] C. Gruian, E. Vanea, S. Simon, V. Simon, FTIR and XPS studies of protein adsorption onto functionalized bioactive glass, Biochim. et Biophysi. Acta 1824 (2012) 873-881.
[48] C. Gruian, E. Vanea, S. Simon, V. Simon, FTIR and XPS studies of protein adsorption onto functionalized bioactive glass, Biochim. et Biophysi. Acta 1824 (2012) 873-881.
[49] A. Balamurugan , G. Sockalingum, J. Michel, J. Fauré, V. Banchet, L. Wortham, S. Bouthors, D. Laurent-Maquin, G. Balossier, Synthesis and characterisation of sol gel derived bioactive glass for biomedical applications, Mat. Let. 60 (2006) 3752-3757.
[50] D.C. Clupper, J.E. Gough, P.M. Ebanga, I.Notingher, L.L.Hench, Bioactive evaluation of 45S5 bioactive glass fibres and preliminary study of human osteoblast attachment, J. mat. Sci.: mat. in med. 15 (2004) 803-808.
[51] E. Saiz, M. Goldman, and A. P. Tomsia, FTIR Analysis of Apatite Formation on Bioactive Glass Coatings on Ti Alloys, Mat. Science Division, Lawrence Berkeley National Laboratory, Berkeley CA 94720
[52] A. El-Ghannam, P. Ducheyne, I.M. Shapiro, Formation of surface reaction products on bioactive glass and their effects on the expression of the osteoblastic phenotype and the deposition of mineralized extracellular matrix, Biomat. 18 (1997) 295-303.
[53] G.A. Stanciu, I. Sandulescu, B. Savu1, S.G. Stanciu1, K.M. Paraskevopoulos, X. Chatzistavrou, E. Kontonasaki, P. Koidis, Investigation of the Hydroxyapatite Growth on Bioactive Glass Surface, J. Biomed.& Pharmaceut.Eng. 1 (2007) 34-39.
[54] H. Wang, J-K Lee, A. Moursi, J J. Lannutti, Ca/P ratio effects on the degradation of hydroxyapatite in vitro, J. Biomed. Mater. Res 67A, (2003)599-608
[55] R. Zhou, S. Si, Q. Zhang, Water-dispersible hydroxyapatite nanoparticles synthesized in aqueous solution containing grape seed extract, Appl. Surf. Sci. 258 (2012) 3578-3583.
[56] G.-C.Yen, P.-D. Duh, H.-L. Tsai, Antioxidant and pro-oxidant properties of ascorbic acid and gallic acid, Food Chem. 79 (2002) 307-313.
[57] A. Kanta, R. Sedev, R. Ralston, Thermally- and photo induced changes in the water wettability of low surface area silica and titania, Langmuir 21 (2005) 2400-2407.
[58] BS Bal, MN Rahaman, Orthopedic applications of silicon nitride ceramics, Acta Biomat. 8 (2012) 2889-2898.
[59] M. Kosmulski, pH dependent surface charging and point of zero charge. IV. Update and new approach, J. Colloid Interface Sci. 337 (2009) 439-448.
[60] T. Luxbacher, The ZETA guide, principles of the streaming potential technique, Anton Paar.
[61] H.H. Lu, S.R. Pollak, P. Ducheyne, Temporal zeta potential variations of 45S5 bioactive glass immersed in electrolyte solution, J. Biomed. Mater. 51 (2000) 80-87.
[62] H.H. Lu, S.R. Pollak, P. Ducheyne, 45S5 bioactive glass surface charge variations and the formation of a surface calcium phosphate layer in a solution containing fibronectin, J. Biomed. Mate. 54 (2001) 454-461.

[63] T. Kokubo, H-M. Kim, M. Kawashita, Novel bioactive materials with different mechanical properties, Biomat. 24 (2003) 2161-2175.
[64] T. Kokubo, S. Yamaguchi, Bioactive titanate layers formed on titanium and its alloys by simple chemical and heat treatments, Open Biomed. Engi. J.9 (2015) 29-41.
[65] C. J. Stephanson, G. Flanagan, Antioxidant capacity of silica hydride: a combinational photosensitization and fluorescence detection assay, Free Radical Biol. Med. 35 (2003) 1129-1137.
[66] Y.Hsu, C.Tsai, W.Chuang, W.Chen, Y.Ho ,F.Lu, Protective effects of silica hydride against carbon tetrachloride-induced hepatotoxicity in mice, Food Chem. Toxicol. 48 (2010) 1644-1653.
[67] S. Verma, A. Singh, A.Mishra, Gallic acid: Molecular rival of cancer, Environ. Toxicol. Pharmacol. 35 (2013) 473-485.
[68] A. van de Wiel, P.H.M. van Golde, H.Ch. Hart, Blessings of the grape, Eur. J. Int. Med. 12 (2001) 484-489.
[69] A.V.S. Perumalla, N.S. Hettiarachchy, Green tea and grape seed extracts - Potential applications in food safety and quality, Food Res. Int. 44 (2011) 827-839.
[70] M. Ndiaye, C. Philippe, H. Mukhta, N. Ahmad, The grape antioxidant resveratrol for skin disorders: Promise, prospects, and challenges, Arch. Biochem. Biophys. 508 (2011) 164-170.
[71] N. Paixão, R. Perestrelo, J.C. Marques, J.S. Câmara, Relationship between antioxidant capacity and total phenolic content of red, rose´ and white wines, Food Chem. 105 (2007) 204-214.
[72] A. K. Atoui , A. Mansouri, G. Boskou , P. Kefalas, Tea and herbal infusions: Their antioxidant activity and phenolic profile, Food Chem. 89 (2008) 27-36.
[73] C. J. Dufresne, E. R. Farnworth, A review of latest research findings on the health promotion properties of tea, J. Nut. Biochem. 12 (2001) 404-421.
[74] S.Lin , E.Liu , J. Mau, Effect of different brewing methods on antioxidant properties of steaming green tea, Food Sci. Tech. 41 (2003) 1616-1623.

Figures and tables legend

Figure 1: Gallic acid and natural polyphenols amount expressed in GA equivalent for the uptake solutions (a) and for the samples (b).

Figure 2: XPS high resolution spectra of the carbon region.

Figure 3: XPS high resolution spectra of the oxygen region.

Figure 4: IR spectra of glass powder before and after functionalization with polyphenols after different times of soaking in SBF.

Figure 5: FESEM micrographs of bulk samples.

Figure 6: Contact angle measurements on samples of CEL2 washed and on CEL2 functionalized with GA, GPH and TPH.

Figure 7: a) Zeta potential vs pH in 0.05 M KCl, b) Zeta potential vs time in SBF.

Figure 8: Scavenging activity towards HO• generated by photolysis of H_2O_2 of buffered suspensions of CEL2 washed (blue bar), CEL2+GA (red bar), CEL2+GPH (green bar) and CEL2+TPH (violet bar) in the presence of DMPO as spin trap molecule. The same experiment in the absence of the dust was carried out as positive control (ctrl + , grey bar). The results are expressed as the mean value ± SD of two different determinations. (vs ctrl+: *$p < 0.05$; vs CEL2 washed: #$p < 0.05$).

Table 1: Acronyms and brief description of samples.

Table 2: ion concentration of the SBF used for apatite-forming ability tests.

Table 3: pH values of the solutions of functionalization and of uptake.

Table 4: Atomic percentages of elements from XPS survey analyses detected on samples. (Uncertainty of measurements 0.5-1% at)

Table 5: (a) EDS results of the bulk samples after 7 and 14 days of soaking in SBF. (b) Ca/P ratio of the of the bulk samples after 7 and 14 days of soaking in SBF. (Uncertainty of measurements 1% at)

Table 6: Zeta potential measurements in KCl and SBF, main results.

Figure 1

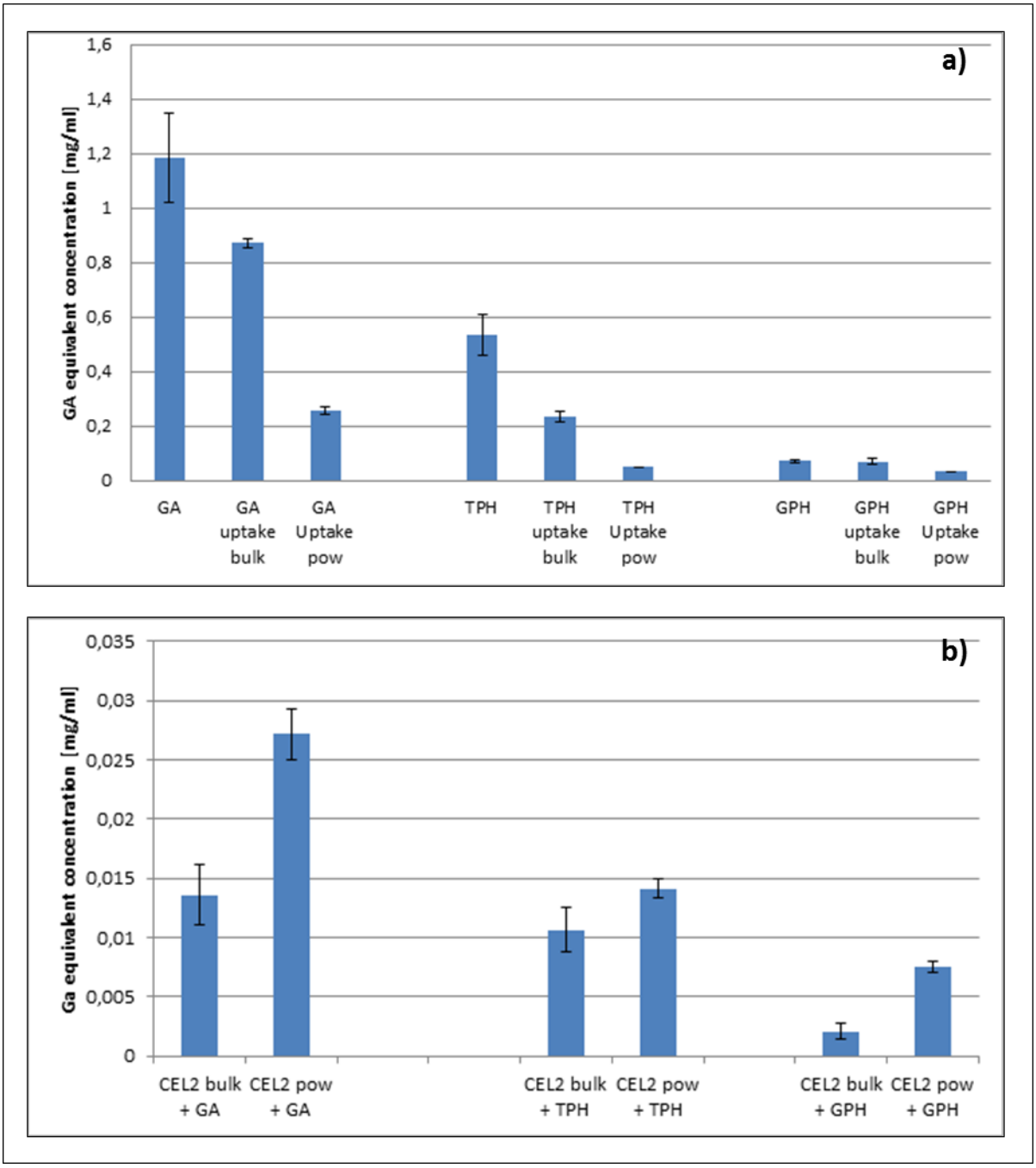
a)
GA equivalent concentration [mg/ml]
1,6
1,4
1,2
1
0,8
0,6
0,4
0,2
0
GA
GA uptake bulk
GA Uptake pow
TPH
TPH uptake bulk
TPH Uptake pow
GPH
GPH uptake bulk
GPH Uptake pow
b)
Ga equivalent concentration [mg/ml]
0,035
0,03
0,025
0,02
0,015
0,01
0,005
0
CEL2 bulk + GA
CEL2 pow + GA
CEL2 bulk + TPH
CEL2 pow + TPH
CEL2 bulk + GPH
CEL2 pow + GPH

Figure 2

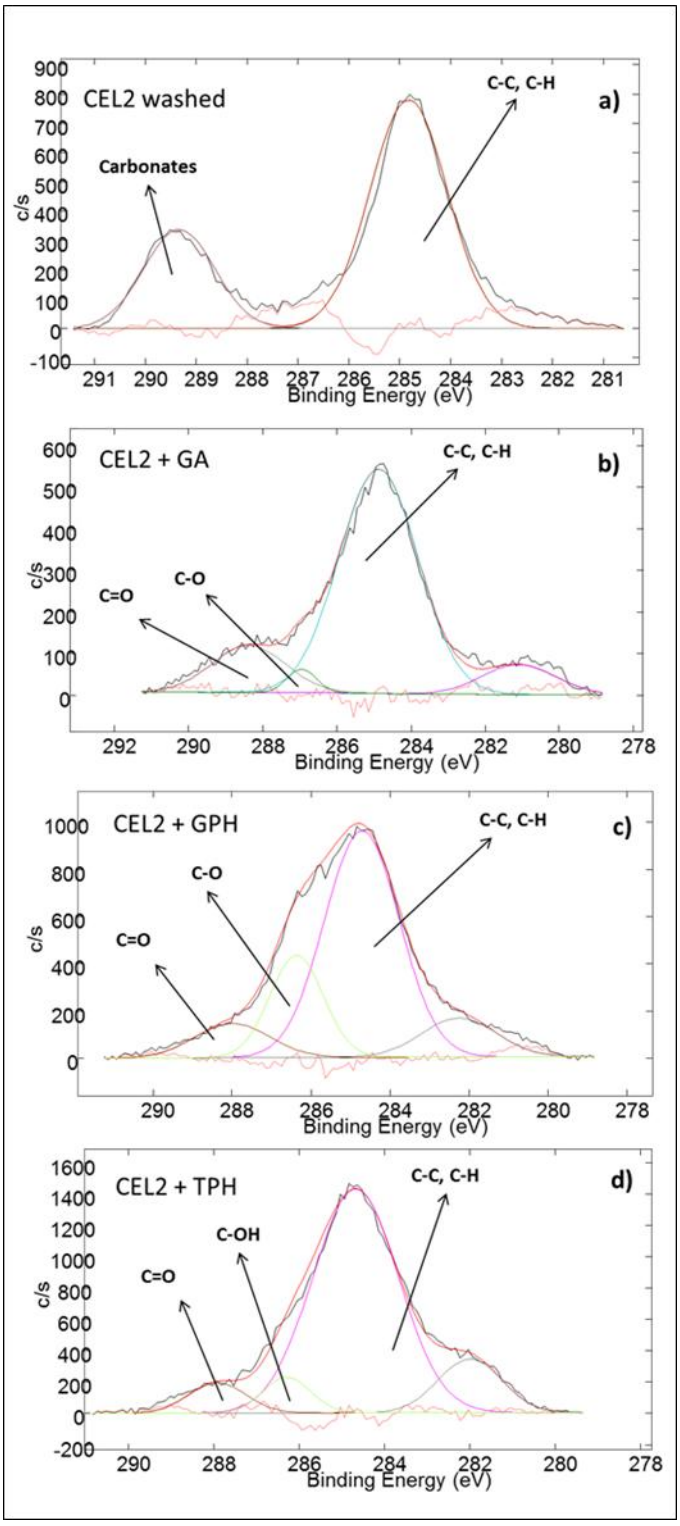
CEL2 washed
a)
C-C, C-H
Carbonates
c/s
Binding Energy (eV)
CEL2 + GA
b)
C-C, C-H
C-O
C=O
c/s
Binding Energy (eV)
CEL2 + GPH
c)
C-C, C-H
C-O
C=O
c/s
Binding Energy (eV)
CEL2 + TPH
d)
C-C, C-H
C-OH
C=O
c/s
Binding Energy (eV)

Figure 3

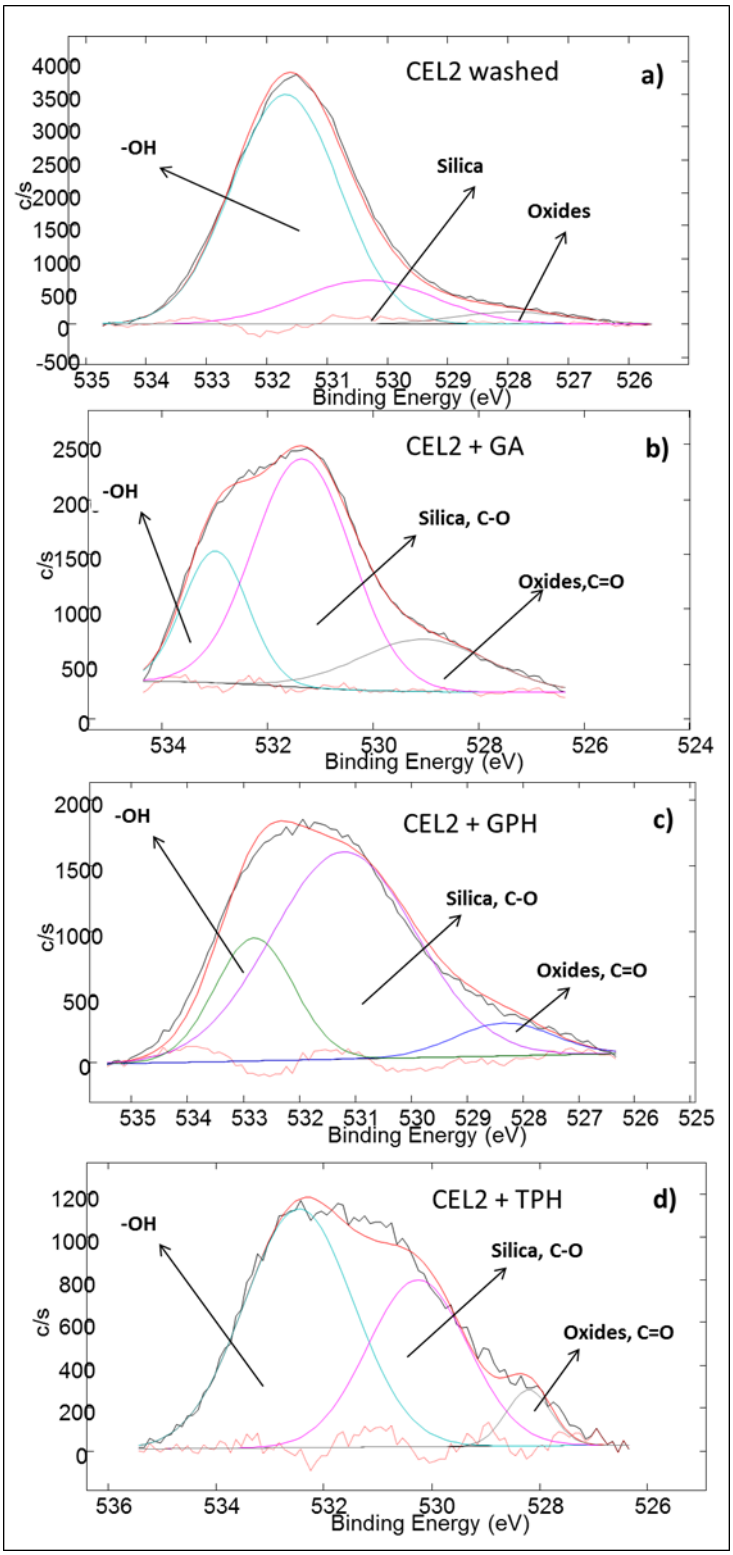
CEL2 washed
a)
-OH
Silica
Oxides
c/s
Binding Energy (eV)
CEL2 + GA
b)
-OH
Silica, C-O
Oxides,C=O
c/s
Binding Energy (eV)
CEL2 + GPH
c)
-OH
Silica, C-O
Oxides, C=O
c/s
Binding Energy (eV)
CEL2 + TPH
d)
-OH
Silica, C-O
Oxides, C=O
c/s
Binding Energy (eV)

Figure 4

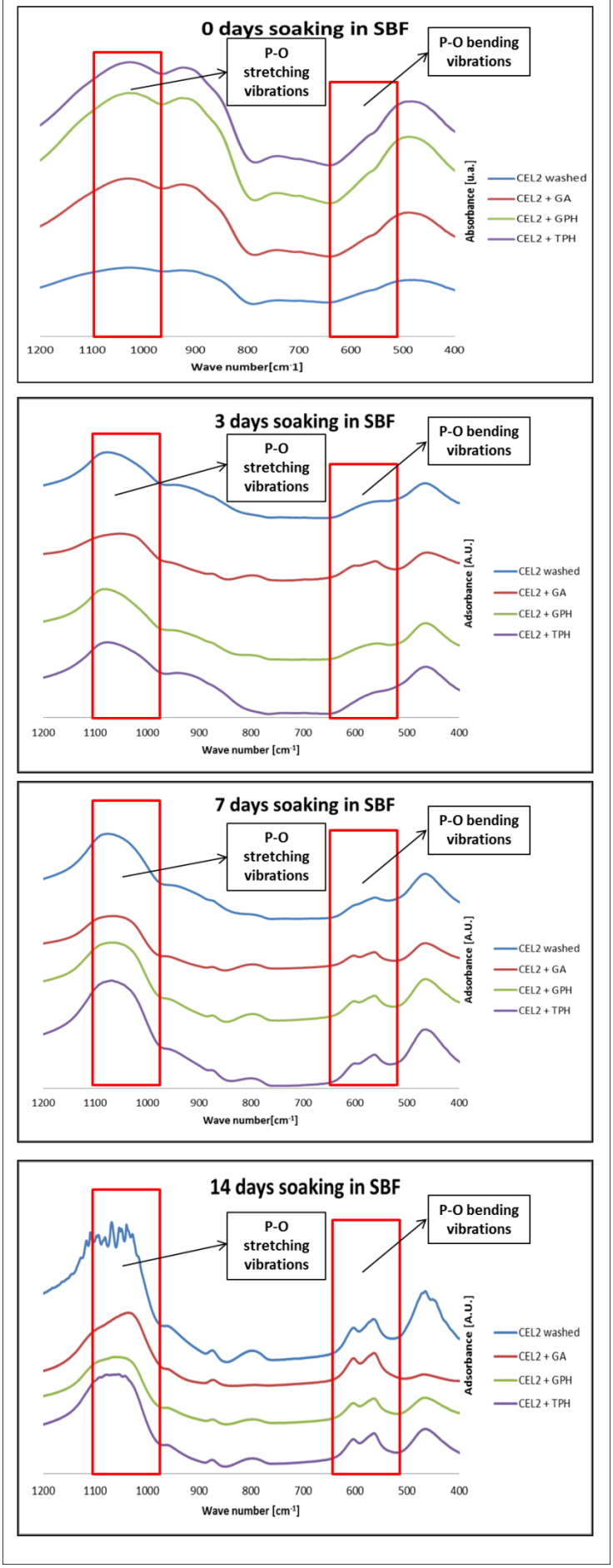
0 days soaking in SBF
P-O stretching vibrations
P-O bending vibrations
Absorbance [u.a.]
CEL2 washed
CEL2 + GA
CEL2 + GPH
CEL2 + TPH
1200 1100 1000 900 800 700 600 500 400
Wave number[cm-1]
3 days soaking in SBF
P-O stretching vibrations
P-O bending vibrations
Adsorbance [A.U.]
CEL2 washed
CEL2 + GA
CEL2 + GPH
CEL2 + TPH
1200 1100 1000 900 800 700 600 500 400
Wave number [cm-1]
7 days soaking in SBF
P-O stretching vibrations
P-O bending vibrations
Adsorbance [A.U.]
CEL2 washed
CEL2 + GA
CEL2 + GPH
CEL2 + TPH
1200 1100 1000 900 800 700 600 500 400
Wave number[cm-1]
14 days soaking in SBF
P-O stretching vibrations
P-O bending vibrations
Adsorbance [A.U.]
CEL2 washed
CEL2 + GA
CEL2 + GPH
CEL2 + TPH
1200 1100 1000 900 800 700 600 500 400
Wave number [cm-1]

Figure 5

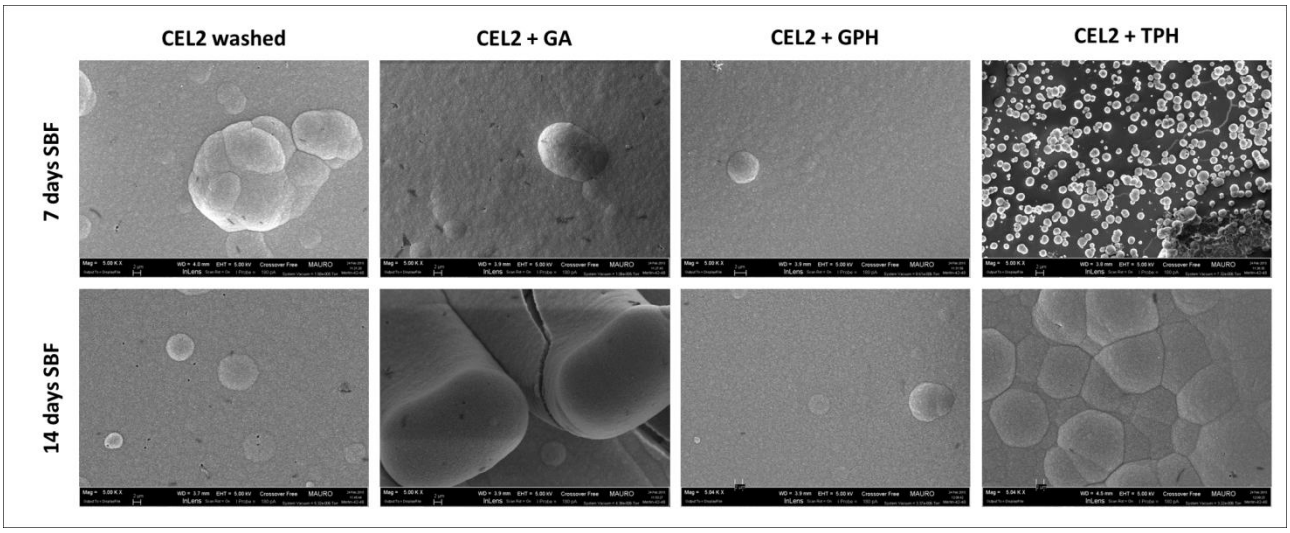

Figure 6

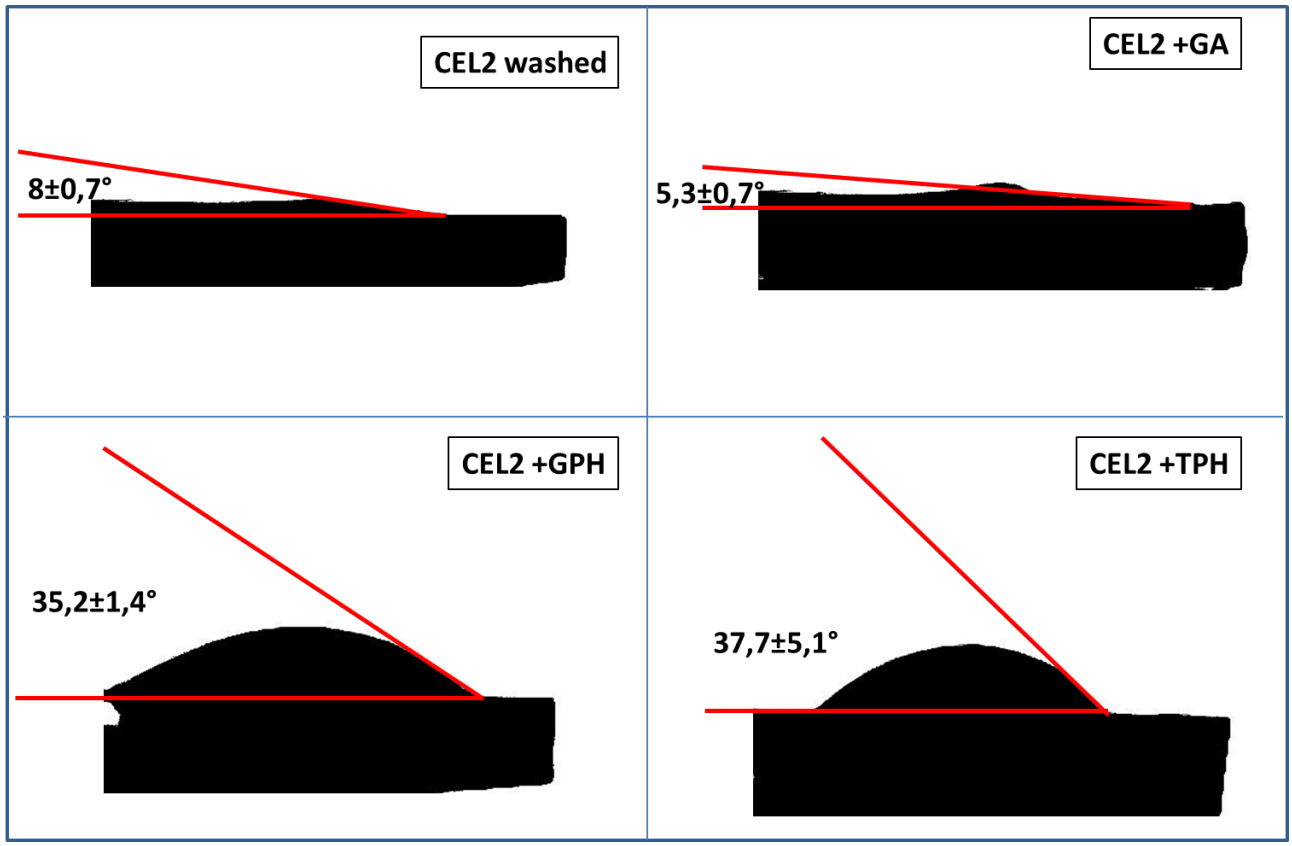

Figure 7

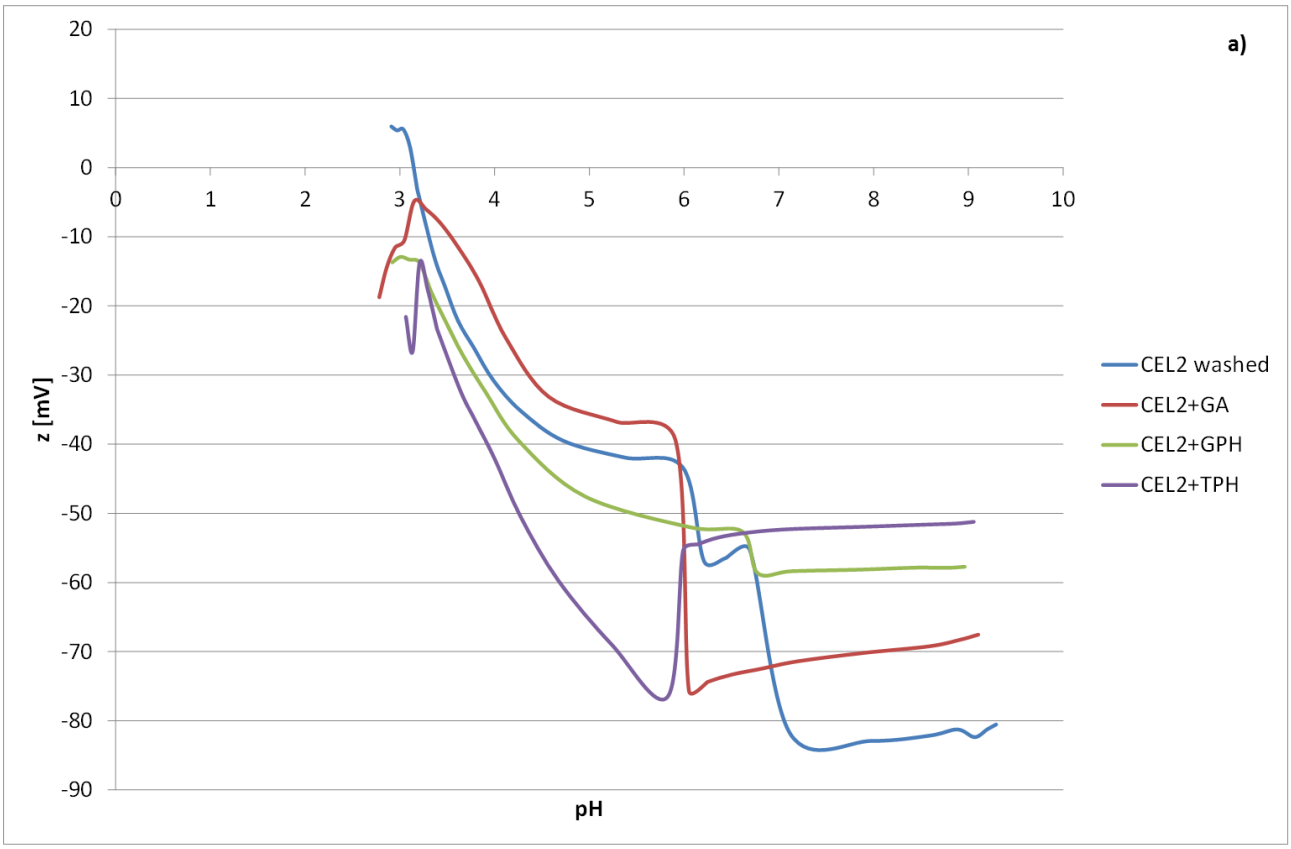
a)
20
10
0
-10
-20
-30
-40
-50
-60
-70
-80
-90
0
1
2
3
4
5
6
7
8
9
10
z [mV]
pH
CEL2 washed
CEL2+GA
CEL2+GPH
CEL2+TPH

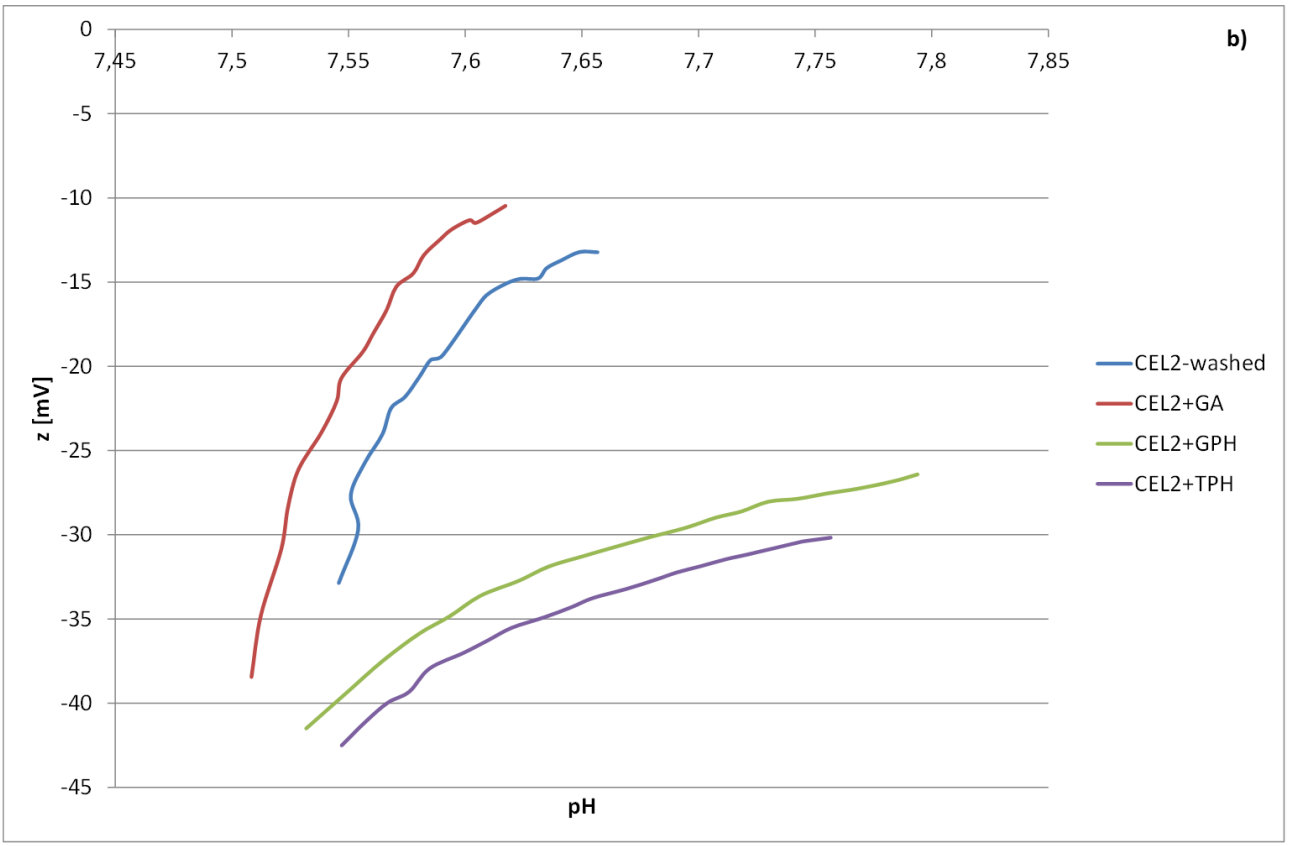
b)
0
-5
-10
-15
-20
-25
-30
-35
-40
-45
7,45
7,5
7,55
7,6
7,65
7,7
7,75
7,8
7,85
z [mV]
pH
CEL2-washed
CEL2+GA
CEL2+GPH
CEL2+TPH

Figure 8

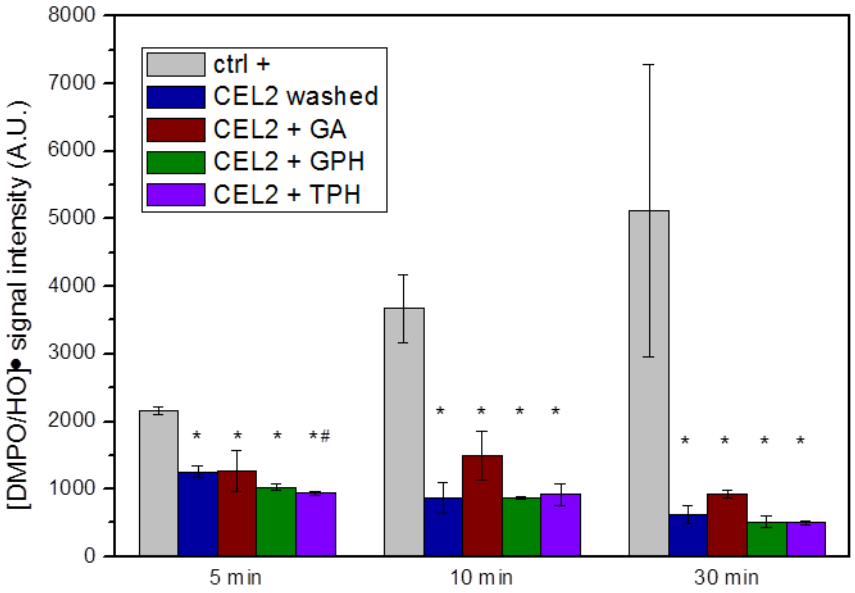
8000
7000
6000
5000
4000
3000
2000
1000
0
[DMPO/HO]• signal intensity (A.U.)
ctrl +
CEL2 washed
CEL2 + GA
CEL2 + GPH
CEL2 + TPH
*
*
*
*#
*
*
*
*
*
*
*
*
5 min
10 min
30 min

Tables

Sample acronym	Sample description
GA	Gallic acid
GPH	Grape polyphenols
TPH	Tea polyphenols
CEL2 washed	CEL2 washed (acetone and water)
CEL2+GA	CEL2 functionalized with gallic acid
CEL2+GPH	CEL2 functionalized with grape polyphenols
CEL2+TPH	CEL2 functionalized with tea polyphenols

Ion concentration in SBF [mM]							
Na^+	K^+	Mg^{2+}	Ca^{2+}	Cl^-	HCO_3^-	HPO_4^{2-}	SO_4^{2-}
142,0	5,0	1,5	2,5	147,8	4,2	1,0	0,5

Solution	pH	Color of the solution
GA	3.25 ± 0.08	Colorless
GA + CEL2 bulk	4.66 ± 0.17	Colorless
GA + CEL2 pow	8.84 ± 0.15	Colored
GPH	3.89 ± 0.34	Colored
GPH + CEL2 bulk	5.62 ± 0.45	Colored
GPH + CEL2 pow	10.71 ± 0.20	Colored
TPH	4.60 ± 0.36	Colored
TPH + CEL2 bulk	7.71 ± 0.18	Colored
TPH + CEL2 pow	9.67 ± 0.09	Colored

	Samples			
Elements [%at]	**CEL2 washed**	**CEL2+GA**	**CEL2+GPH**	**CEL2+TPH**
O	50,9	58,2	40,7	28
C	30,3	26,1	49	67,6
Si	6,6	11,4	2,5	-
Ca	5,4	-	3,7	1,7
Na	4,6	1,1	2,1	1,6
P	1,4	3,3	2,0	0,9
K	0,8	-	-	-
Mg	<0,1	<0,1	<0,1	0,2

(a)

	Samples							
	CEL2 washed		CEL2 + GA		CEL2 + GPH		CEL2 + TPH	
Elements (weight %)	*7 days soaking*	*14 days soaking*	*7 days soaking*	*14 days soaking*	*7 days soaking*	*14 days soaking*	*7 days soaking*	*14 days soaking*
C	7,26	5,76	5,11	4,79	5,42	7,97	9,37	5,14
O	64,24	54,42	54,62	52,55	58,09	56,05	50,62	54,86
Na		0,64	-	-	-	-	-	-
Mg	0,93	0,64	0,8	0,8	0,74	0,77	1,94	1,15
Si	-	-	-	-	-	-	4,98	-
P	9,52	12,08	11,37	12,12	11,09	11,37	10,54	12,72
Ca	13,03	21,64	21,76	23,44	18,83	18,54	17,85	21,14
Cr	5,02	4,81	6,33	6,3	5,82	5,31	4,7	4,99

(b)

	Samples							
	CEL2 washed		CEL2 + GA		CEL2 + GPH		CEL2 + TPH	
	7 days soaking	*14 days soaking*	*7 days soaking*	*14 days soaking*	*7 days soaking*	*14 days soaking*	*7 days soaking*	*14 days soaking*
CA/P ratio	1,3686975	1,791391	1,913808	1,933993	1,697926	1,630607	1,693548	1,66195

	Measurements in 0.05 M KCl		Measurements in SBF			
			Cycle 0		Cycle 20	
	IEP	Z [mV] (pH≈7.5)	pH	Z [mV]	pH	Z [mV]
CEL2 washed	3.12±0.1	-82±26	7.55±0.00	-33±5	7.66±0.00	-13±6
CEL2+GA	n.d.	-70±0	7.51±0.00	-38±5	7.62±0.00	-10±17
CEL2+GPH	n.d.	-58±0	7.53±0.00	-41±1	7.79±0.00	-26±3
CEL2+TPH	n.d.	-52±1	7.55±0.00	-42±0	7.76±0.00	-30±2

n.d. = not determined